



ARTICLE

# Corona with Streamers in Atmospheric Pressure Air in a Highly Inhomogeneous Electric Field

**Victor Tarasenko\* Evgenii Baksht Vladimir Kuznetsov Victor Panarin Victor Skakun  
Eduard Sosnin Dmitry Beloplotov**

Institute of High Current Electronics, Siberian Branch (SB), Russian Academy of Sciences (RAS), 2/3 Akademicheskii Ave., Tomsk, 634055, Russia

ARTICLE INFO

*Article history*

Received: 2 September 2020

Accepted: 7 September 2020

Published Online: 30 September 2020

*Keywords:*

Positive and negative coronas

Atmospheric pressure air

Highly inhomogeneous electric field

ICCD camera

Ball streamer

Cylindrical streamer

ABSTRACT

The paper presents research data on positive and negative coronas in atmospheric pressure air in a highly inhomogeneous electric field. The data show that irrespective of the polarity of pointed electrodes placed in a high electric field (200 kV/cm), this type of discharge develops via ball streamers even if the gap voltage rises slowly (0.2 kV/ms). The start voltage of first positive streamers, compared to negative ones, is higher and the amplitude and the frequency of their current pulses are much lower: about two times and more than two orders of magnitude, respectively. The higher frequency of current pulses from negative streamers provides higher average currents and larger luminous areas of negative coronas compared to positive ones. Positive and negative cylindrical streamers from a pointed to a plane electrode are detected and successive discharge transitions at both polarities are identified.

## 1. Introduction

Corona discharges in air and other gases at different pressures continue to attract the attention of researchers<sup>[1-25]</sup>. Coronas are a self-sustained discharge arising near an electrode or electrodes with a small radius of curvature<sup>[26,27]</sup>. Typically, two main areas appear in this type of discharge: an ionization region near a pointed electrode where the electric field is high and a region remote from it where the field is low and the current is provided by charged particle drift. As has recently been proven<sup>[28]</sup>, the part of current in non-ionized region

is contributed by dynamic displacement current due to fast plasma expansion by streamers from a pointed electrode. Corona discharges can be initiated by applying DC and AC voltages and by applying short voltage pulses which make them short-lived in a single form<sup>[5,7,13]</sup>.

Coronas can be positive or negative depending on the voltage polarity of pointed electrodes<sup>[1-27]</sup>. Negative coronas can produce current pulses hundred nanoseconds long whose frequency increases with voltage<sup>[26,27]</sup>. Such corona bursts are known as Trichel pulses<sup>[29]</sup>, and in some studies, they are related to negative streamers<sup>[18,20,24]</sup>. Data are also available on how this type of discharge near a negative electrode is

\*Corresponding Author:

Victor Tarasenko,

Institute of High Current Electronics, Siberian Branch (SB), Russian Academy of Sciences (RAS), 2/3 Akademicheskii Ave., Tomsk, 634055, Russia;

Email: [VFT@loi.hcei.tsc.ru](mailto:VFT@loi.hcei.tsc.ru)

transformed and constricted<sup>[4]</sup>. Positive coronas can produce cylindrical jets<sup>[7]</sup> whose length increases greatly if an additional ring electrode is present in their region<sup>[22]</sup>. The threshold current for corona-to-glow and glow-to-spark transitions can vary with the geometry of an anode, its resistivity, length of gap, and gas flow<sup>[3]</sup>. The start voltage of positive coronas, compared to negative ones, is higher<sup>[4,20,26,27]</sup>.

Despite abundant research data on corona discharges, their studies are continued<sup>[17-25,30]</sup>. In particular, some features of coronas remain unclear. For example, if the gap voltage rises slowly, lower voltages are needed for a negative corona<sup>[4,20]</sup>. At the same time, the electric field needed for a negative streamer is about twice that for a positive one:  $\sim 10 \text{ kV/cm}^2$  against  $5 \text{ kV/cm}^2$  in atmospheric pressure air<sup>[27]</sup>. Thus, the question arises of why corona discharges appear earlier at negative polarity and cylindrical streamers at positive. This and other features of corona discharges are still poorly understood. From the available data, it is unclear whether the first current pulses of negative and positive coronas can be related to the formation of streamers.

Only recently<sup>[20,30]</sup> it has been found that the initiation of corona discharges can start with the formation of a streamer with a large diameter at both voltage polarities. Such streamers propagated from needle electrodes with a tip radius of tens of microns at a slowly rising voltage<sup>[20, 30]</sup>. Note that in some studies<sup>[31,32]</sup>, such streamers produced by nanosecond voltage pulses were termed broad or wide, and they were really wide, reaching 8 cm in diameter at high rates of rise of voltage ( $dU/dt > 10^{14} \text{ kV/ns}$ ).

All the foregoing suggests that further research in the features of coronas is needed. In the paper presented, we analyze the initiation of corona discharges from electrodes with a small radius of curvature in point-plane gaps and the conditions for their transition to other forms at both voltage polarities with a minimal voltage of less than 2 kV.

## 2. Experimental Setup and Measuring Techniques

The experimental setup for research in corona discharges in atmospheric pressure air comprised a power supply, a point-plane electrode gap, and a measuring system (Figure 1).

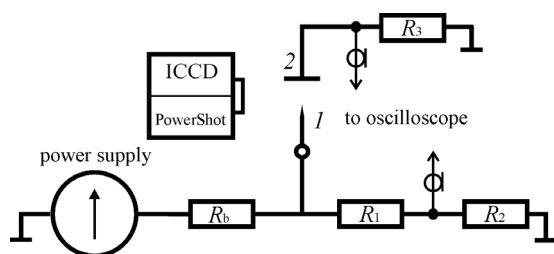


**Figure 1.** Experimental setup:  $R_b = 18 \text{ MOhm}$ ,  $R_1 = 2.5 \text{ MOhm}$ ,  $R_2 = 2.5 \text{ kOhm}$ ,  $R_3 = 1 \text{ kOhm}$

For assessing the minimum start voltage of coronas, we used a high-voltage source with a voltage stability and long needles with a small radius of curvature (Table 1).

**Table 1.** Needle parameters

Size	Diameter, mm	Tip radius, $\mu\text{m}$
No. 1a	0.32	11-13
No. 1b	0.32	40
No. 2	0.61	30
No. 3	1.04	100
No. 4	3	200

Most of the experiments were performed with a beading needle of size No. 1a having a tip radius of 11-13  $\mu\text{m}$ , length of 55 mm, and diameter of 0.32 mm. Because the tip of needle No. 1a during high-voltage operation was melted and its radius increased up to  $\approx 40 \mu\text{m}$  (needle No. 1b), the needle was regularly replaced by a fresh one. The tips of the other needles (Nos. 2, 3, 4) after spark breakdowns were less eroded but their radius was also increased. The least increase in the tip radius was observed for needle No. 4. The material of needle No. 4 was copper, and that of needles Nos. 1, 2, 3 was stainless steel.

The second (grounded) electrode was plane, allowing current measurements. The distance between the tip of a needle and plane electrode was varied from 2 to 50 mm. Because needle No. 1a was subjected to strong corona vibrations due to its small diameter and large length, its tip was fixed with a teflon plate to reliably capture the discharge form. Several experiments were performed only with a needle (and with no shunt) for which all grounded metal conductors were spaced from it by more than 10 cm.

In our experiments, we used three voltage sources: (1) a source with a stabilized voltage of 0.4- 5 kV accurate to no worse than 0.2% and with a rate of voltage rise no greater than 0.2 kV/ms; (2) a source with a voltage of up to 36 kV and rate of voltage rise of no more than 0.2 kV/ms; (3) and a source with sinusoidal voltage pulses of both polarities rising up to 20 kV in  $\approx 500 \text{ ns}$ .

The form of corona discharges was captured in frame-by-frame mode with a Canon PowerShot SX 60 HS camera and was recorded with an HSFC PRO four-channel ICCD camera at a minimum frame duration of 3 ns.

The time dependence of voltage was traced with a high-voltage probe and a Tektronix TDS 3034 oscilloscope. The discharge current measured by a high-resistance shunt ( $R = 1 \text{ kOhm}$ ) was recorded with a resolution of no worse than 5 ns. Thus, we could measure the pulsed and steady component of the current through the gap. All experiments were performed in a laboratory room in am-

bient air at a temperature of  $\approx 20$  °C and humidity of no more than 60%.

### 3. Experimental Results

#### 3.1 Current-voltage Characteristics of Corona Discharges

Despite numerous experimental studies of corona discharges, no complex analysis is available to judge their evolution. In particular, little is known about the early stage of coronas, the more so as their studies with high time resolution are comparatively rare. In our study, we have analyzed the relationship between the characteristics of coronas and modes of their operation. Figure 2 shows the average discharge current versus the voltage of both polarities at the tip of needle No. 4.

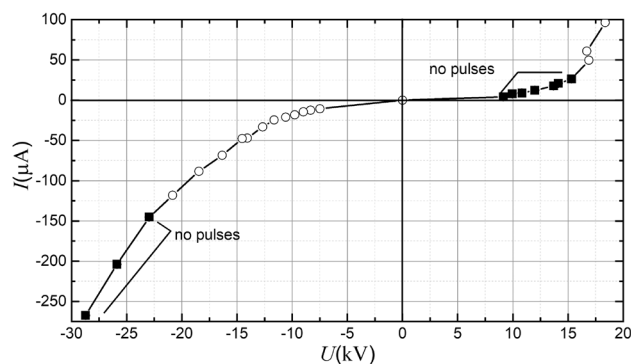


**Figure 2.** Average discharge current versus negative and positive polarity voltage with needle No. 4 spaced from plane electrode by 20 mm

Needle No. 4 was used because its tip was little affected by several sparks while the tips of needles Nos. 1, 2, 3 were blunted. The average current was determined through oscilloscope measurements for 400  $\mu$ s. Each point in Figure 2 was obtained at constant voltage. During the measurement time (400  $\mu$ s), short current pulses were recorded (open circles on the diagram). At the same voltage level, their frequency at negative polarity was more than an order of magnitude greater than its value at positive polarity. Thus, the discharge current on the diagram is represented by its quasi-steady and pulsed components.

The current-voltage characteristics in Figure 2 are typical for corona discharges: higher discharge start voltages and lower average discharge currents at positive than at negative voltage polarity. The oscilloscope recorded the corona current and the gap voltage simultaneously at each measurement point, allowing us to identify pulsed, quasi-steady, and mixed modes of the current flow at each voltage (by varying the time sweep) and to determine the frequency of current pulses, their amplitude, and duration.

The pulsed mode was always observed at initiation of

corona discharge. Previous studies showed that the pulsed mode is related with the formation of spherical (wide) streamers in the vicinity of a needle<sup>[20]</sup>.

At both voltage polarities, a quasi-steady discharge mode (free of individual pulses during 400  $\mu$ s) was observed. At positive polarity, the voltage for this mode was relatively lower than at negative polarity. Over time, the quasi-steady mode transformed to a mixed one. This mode comprised two components: quasi-steady and pulsed. At positive polarity, the contribution from individual pulses to the mixed mode was negligible. At negative polarity, such a mode with its quasi-steady component and Trichel pulses<sup>[26,29]</sup> was observed with increasing voltage after the start of a corona. For negative polarity, the voltage at which current pulses with a relatively high frequency appeared was about 7.5 kV (Figure 2). For positive polarity, it was higher. When voltage of any polarity was increased greatly, the corona transformed to a glow and then to a spark discharge.

The waveforms of voltage and current were recorded not only at constant voltages but also at voltage rise time and fall time from tens of milliseconds to several seconds. As for the average corona current, the current-voltage characteristics at relatively short voltage rise and fall times differed little from those at constant voltages. However, it was possible to observe all modes and transitions of corona discharge.

Figure 3 shows the waveforms of voltage and current of a negative corona recorded within 35 ms when applying needle No. 1b.

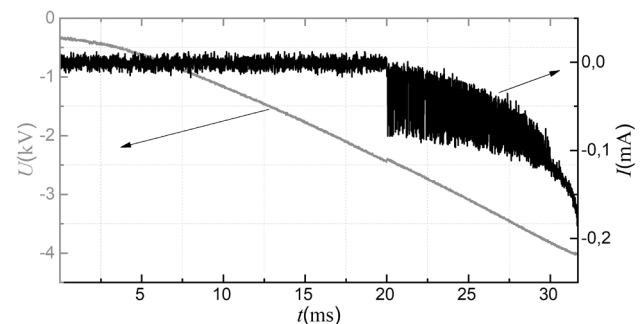


**Figure 3.** Waveforms of voltage and current of negative corona recorded from within  $\sim 35$  ms. Needle No. 1b. Length of gap 3 mm

Until  $\approx 20$  ms (Figure 3), the current through the gap was low ( $< 1$   $\mu$ A) and corresponded to dark current due to air ionization by high-energy cosmic particles<sup>[27]</sup>. Once a negative corona was ignited ( $\approx 2.2$  kV), Trichel pulses and then quasi-steady component appeared. The quasi-steady component increased with increasing the voltage while the amplitude of current pulses decreased (if counted from the quasi-steady level) such that they became undetectable

at  $\approx 3.1$  kV. We think that it is the onset of corona-to-glow discharge transition. The transition was accompanied by electron emission from a bright cathode spot and gradual extension of the corona current-voltage characteristic into a glow one. Further increasing the voltage gave rise to a spark discharge such that the gap voltage dropped and the current increased significantly. Transforming the spark to a corona or a glow discharge required a decrease in the power supply voltage. All these modes can be judged from their respective waveforms and images in the sections below.

Figure 4 shows the waveforms of voltage and current of a positive corona when applying needle No. 1b. When the needle was positive, the current got quasi-steady after the first pulse and remained quasi-steady during  $>400$   $\mu$ s. The mixed mode was observed only at relatively high voltages.

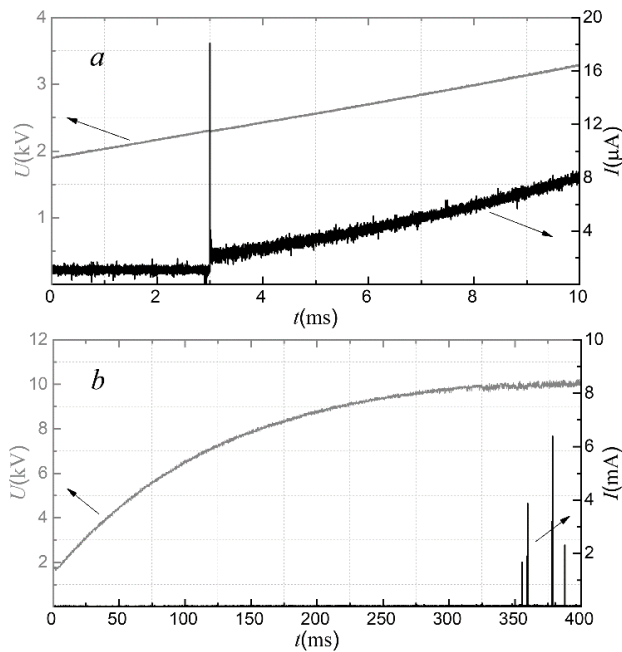


**Figure 4.** Waveforms of voltage and current of positive corona when applying needle No. 1b. Length of gap 10 mm

The positive corona developed via ball streamers. The appearance of the ball streamer in the vicinity of the needle tip is accompanied by a short current pulse (Figure 4a) after which the discharge became quasi-steady and its average current increased with increasing the voltage. In the quasi-steady mode, pulses were also possible but their frequency was too low to make them full-blown. The high amplitude of the current pulse is due to the high rate of ionization processes in the vicinity of the needle tip, where the electric field strength is very high. The short duration of the current pulse is caused by a rapid decrease

in the rate of ionization processes as the diameter of the streamer increases and the strength of the electric field at its front decreases. These features of current during the development of a streamer were studied in [28].

At a higher voltage ( $\approx 10$  kV, Figure 4b), the positive corona revealed cylindrical streamers [30]. As can be seen in Figure 4b, cylindrical streamers are also accompanied by current pulses. Their amplitude and duration are greater than that for the ball streamers formed in the vicinity of the needle tip at lower voltages. The voltage practically does not change. It drops when the discharge transforms to a spark with increasing the power supply voltage. As has been shown [26], lower values of slowly rising voltage in an inhomogeneous electric field are needed for a spark breakdown from positive pointed electrodes compared to negative ones. Our study confirms this conclusion (Figure 2).

### 3.2 Initiation of Coronas

Let us look closer at the initiation of corona discharges. Our previous studies [20,30] show that the initiation of a corona starts with a ball streamer not only at negative but also at positive voltage polarity. In particular, such a streamer is identified from current pulses with a duration of 100-200 ns recorded by a current shunt and from plasmas appearing at pointed electrodes during this time. In negative coronas, such current pulses are frequent [26,29]. The detection of current pulses with a duration of 100-200 ns in positive coronas is reported elsewhere [20].

Our detailed study confirms that corona discharge in a highly inhomogeneous electric field is initiated at a comparatively low voltage which, as expected, increases with increasing the tip radius and diameter of a needle. The start voltages of corona discharge for needles of different sizes and point-plane gaps of different widths are indicated in Table 2.

**Table 2.** Corona start voltage for different needles

Needle size	Voltage polarity	Gap, cm	Corona start voltage, kV
No. 1b	+	3	6.0
No. 2b	+	3	7.0
No. 2b	+	1	3.8
No. 2b	+	2	4.2
No. 3b	+	3	10.0
No. 3b	-	3	6.5

When going from positive to negative polarity, the start voltage of corona decreases with decreasing the gap width  $d$  and increases with increasing the tip radius and needle diameter. The data in Table 2 are for needles with

spark-blunted tips (index b) and hence with higher corona start voltages compared to sharp ones, all other things being equal.

The initiation of corona at minimal voltages was studied with needle No. 1a having the smallest tip radius (11  $\mu\text{m}$ ). When the tip was blunted, the needle was replaced by a fresh one. Such pointed electrodes were needed to produce the highest electric field and to initiate single streamers at low voltages. The power supply was stabilized. Figure 5 shows the start voltage of first streamers versus the gap between needle No. 1a and plane electrode.

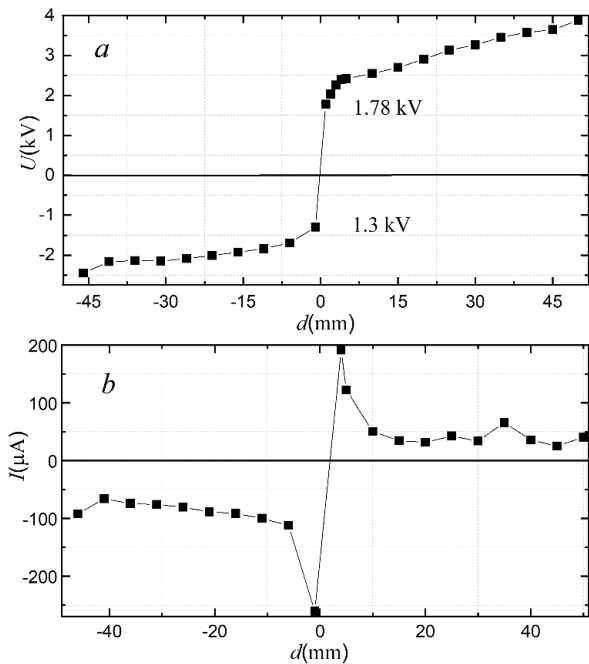


**Figure 5.** Start voltage of first current pulses (a) and their amplitude (b) versus gap  $d$  between needle No. 1a and plane electrode. Negative  $d$  values are for negative voltage polarity

With sharp needles No.1a, like with blunted ones, the corona start voltage was lower at negative than at positive polarity. Besides, the start voltage of first pulses at positive polarity, compared to negative one, increased faster with  $d$ . It should also be noted that although the start voltage of first current pulses increased with  $d$ , the current amplitude decreased (Figure 5b). These data are apparently new.

Figure 6 shows the waveforms of first current pulses and pulses in mixed modes at positive and negative voltage polarity for needle No.1b. The time resolution is no worse than 5 ns.

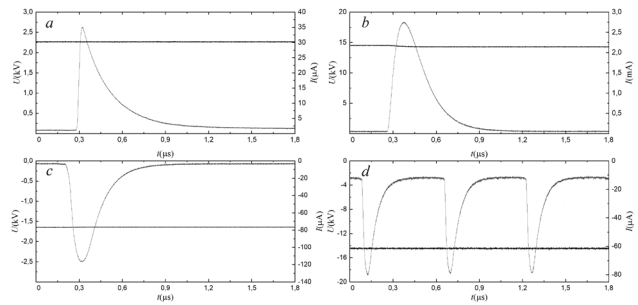


**Figure 6.** First current pulses (a, c) and pulses in mixed modes (b, d) at different voltages (straight lines) at positive (a, b) and negative polarity (c, d). Gaps 5 (a, c) and 40 mm (b, d). Needle No. 1b

As can be seen, the start voltage of first pulses with  $d = 5$  mm is 1.64 kV at negative and 2.26 kV at positive polarity, which agrees with the data of Figure 5a. The waveforms in Figure 6a,c also suggest that at positive polarity, compared to negative polarity, the rise time of the pulse is shorter but its fall time is longer and its width at a level of 0.1 is larger. Increasing the gap to 40 mm increases the start voltage and the amplitude of first current pulses.

It should be noted that the start voltage and the current of coronas depend on not only the tip radius and length of gap but also on the humidity and pressure of air. Our comparative measurements were taken during a short time and under the same weather conditions, and although the parameters did vary from day to day (primarily due to varying air humidity), their tendencies remained unchanged.

The amplitude of pulses and their spacing depended on the voltage and its polarity. At relatively low voltages, the amplitudes of the first corona current pulses are usually larger when a needle electrode is negative. As will be shown below, under these conditions, ball streamers are formed. However, cylindrical streamers are formed from a positive needle with increasing voltage, and the amplitude of the positive corona current pulses increases significantly. For example, at a positive polarity voltage of 8 kV, needle No. 1a, and  $d = 8$  mm, they had an amplitude of 6 mA, FWHM of 220 ns, and repetition period of  $\geq 240 \mu\text{s}$  corresponding to a frequency of  $\approx 4.2$  kHz. With the same gap and voltage at negative polarity, they had an amplitude of 56  $\mu\text{A}$ , FWHM of 94 ns, and frequency of 5 MHz, and their steady current component before the next pulse was  $\approx 42 \mu\text{A}$ . At the same voltage, the pulse repetition frequency for the negative polarity, compared to the positive one, was more than several orders of magnitude higher. As a result, a much higher average corona current was observed at negative polarity. The fact that a train of pulses (Trichel pulses) whose frequency increases with voltage appears in a negative corona after its first pulse is described in many papers. Tables 3 and 4 present data on

the amplitude of current pulses and their frequency and spacing at different voltages of negative and positive polarity for needle No. 1a with  $d = 2$  cm.

**Table 3.** Amplitude of current pulses, pulse frequency, and pulse spacing in negative coronas from needle No. 1a with  $d = 2$  cm

$-U, \text{ kV}$	$I, \mu\text{A}$	$f, \text{ kHz}$	$\tau, \mu\text{s}$
3.1	5.4-6.4	28.6	35
4.1	6-6.8	30	33.5
5	5.4-6.4	71	14.08
6	5.2-6.8	149	6.73
9.2	5-6.4	281	3.56
10.1	4.2-6.4	345	2.9
12	4.4-5	476	2.1

**Table 4.** Amplitude of current pulses, pulse frequency, and pulse spacing in positive coronas from needle No. 1a with  $d = 2$  cm

$+U, \text{ kV}$	$I, \mu\text{A}$	$f, \text{ kHz}$	$\tau, \mu\text{s}$
8.8	144	4.49	222.8
9.9	233	5.41	184.7
10.7	389	5.68	176.2
11.4	501	6.17	162.1
12.2	541	7.34	136.3
12.8	689	7.4	135.1
13	809	7.52	133

As noted above, with increasing voltage, cylindrical streamers are formed from a positive needle, and the amplitude of the positive corona current pulses increases significantly.

We think that the recorded current pulses are due to streamers which, as evidenced by discharge images, can be both ball and cylindrical.

### 3.3 Plasma in Corona Discharges

Our study confirms that in atmospheric pressure air, the start voltage of corona discharge from pointed electrodes measures several kilovolts and that their initiation at any voltage polarity is accompanied by current pulses with a FWHM of 100-200 ns (Figure 6). Because of the low start voltage and amplitude of first corona pulses, the intensity of first streamers is very low and so is the corona intensity near the tip of needles in quasi-steady modes. This makes it difficult to capture the early stage of coronas even with ICCD cameras. Therefore, images of coronas at low voltages (few kilovolts) were taken in the dark at the maximum digital camera sensitivity with long exposure times

(mostly, with 15 s). Figure 7 shows the plasma of negative and positive coronas near needle No. 1a.

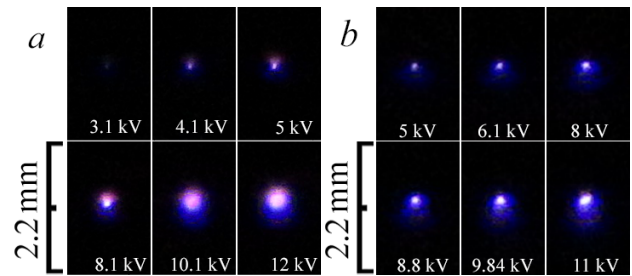


**Figure 7.** Images of corona discharges near needle No. 1a at negative (a) and positive polarity (b). Length of gap 2 cm. Exposure time 15 s

The size of luminous corona areas depended on the voltage and length of gap. At negative polarity, the corona plasma was ball only in the range of low voltages and was contracted as the voltage was increased, which agrees with data reported elsewhere<sup>[4]</sup>. At the same voltage, the total emission near the negative needle, compared to the positive one, was higher. At positive polarity, the plasma was ball over a wider voltage range, and as the voltage was increased, jets escaped from the plasma up to the plane electrode (Figure 8a).

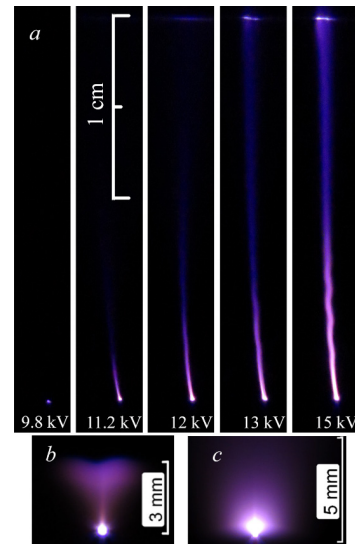


**Figure 8.** Images of discharges from positive needle No. 2b at  $d = 20$  mm (a) and from negative needle No. 1b at  $d = 10$  mm,  $U = 3.8$  kV (b) and negative needle No. 4 at  $d = 10$  mm,  $U = 16.9$  kV (c). Exposure time 15 s

The long jets in Figure 8a are cylindrical positive streamers for which the electric field in gap is two-three times smaller than the field for negative streamers<sup>[27]</sup>. At 15 kV, as can be seen in Figure 8a, such a jet bridges the gap and the corona transforms to a glow discharge which operates stably till the formation of spark channels at high gap voltages. A current-limiting resistor between the

power supply and needle (Figure 1,  $R_b$ ) provides the glow discharge stability at atmospheric pressure. The glow-to-spark discharge transition is fast and voltage across the gap decreases significantly. Such a transition at negative polarity can be judged from Figure 3, and glow discharge at negative polarity from Figs. 8b and 8c, respectively.

Figure 9 shows ICCD images of the plasma of a negative corona near the tip of needle at pulsed voltage.

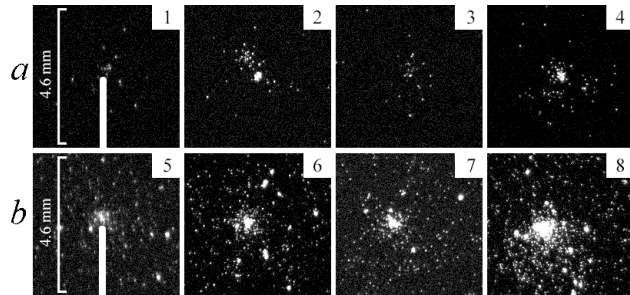


**Figure 9.** ICCD images of negative coronas near needle No. 1b with  $d = 9$  mm at maximum gap voltages 13 kV (a) and 6 kV (b). The needle is shown only in frames 1 and 5. Frame duration 200 ns (1, 2, 3), 600 ns (4), 20  $\mu$ s (5, 6, 7), and 60  $\mu$ s (8) with no time delay between first (1, 5) and second frames (2, 6) and between second and third (3, 7). Last frames (4, 8) are for coronas within respective first frames (1, 2, 3 and 5, 6, 7)

Because of the low intensity and widely varied start time of first streamers at low voltages with low rates of rise, it was impossible to accurately trace their formation dynamics by ICCD imaging. However, an increase in the emission intensity due to streamers was identified in individual frames  $\sim 200$  ns long. As can be seen from Figure 9a, more intense streamer emission is present in frame 2 and in frame 4 whose duration spans that of frames 1, 2, and 3. Such emission within 200 ns corresponds to the current pulse duration of the first ball streamer (Figure 8a, 9.8 kV). Under the conditions considered, the spacing between streamer pulses was much longer than 600 ns, and such images were possible only after tens to hundreds of corona imaging events.

As the frame duration was increased to over 20  $\mu$ s, the detection of individual streamers failed. The emission intensity was determined by the quasi-steady corona current and was the same at the same frame durations. Our experiments on the detection of first streamers at a pulse voltage rise time of 500 ns confirmed the results reported elsewhere<sup>[20]</sup>. Increasing the gap voltage at the rise of first streamers allowed us to capture their emission at negative polarity in frames 200 ns and 100 ns long, which roughly corresponds to the current FWHM through the gap. However, their formation dynamics at such frame durations was untraceable. We think that it is similar to what is ob-

served at voltage pulses of tens of nanoseconds<sup>[32]</sup>. With a frame duration of  $\sim 10$  ns and shorter, the emission intensity of negative streamer was insufficient for its identification, though the total emission intensity at the negative needle, compared to the positive one, was higher due to higher streamer formation rates (Figure 7).

At positive voltage polarity with the same pulse amplitude, we could clarify some details of the formation dynamics of individual streamers. For example, at high voltages, a streamer head moving off the tip was detected in frames of 10 ns. This suggests that increasing the voltage increases the emission intensity of single positive streamers compared to negative ones, which correlates with current pulse amplitudes. In Figure 6a, b, the current pulse amplitudes at different polarities are about equal, and in Tables 3, 4, they are much higher at positive polarity. Such a mode is observed during the formation of cylindrical positive streamers (Figure 8a) from the plasma created at the needle tip by a ball streamer (Figure 7b). Figure 10 shows ICCD images of a cylindrical positive streamer at a constant gap voltage.

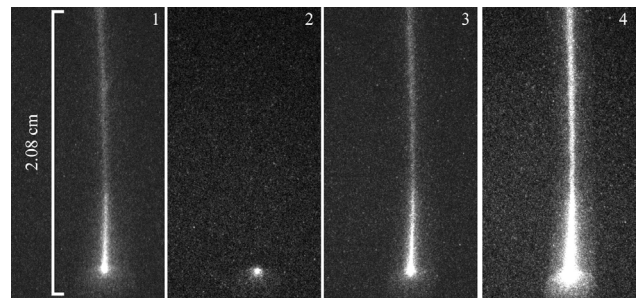


**Figure 10.** ICCD images of cylindrical positive streamer from needle No. 1b with  $d = 21$  mm at maximum gap voltage 17.3 kV. Frame durations 100  $\mu$ s (1, 2, 3) and 300  $\mu$ s (4) with no time delay between first (1) and second frame (2) and between second and third (3). Last frame (4) is for discharge within first three frames.

As can be seen in Figure 10, such a streamer is captured in frames 1 and 3 due to their large spacing, and in frame 4, two cylindrical streamers are overlapped. With no cylindrical streamer in frame 2, only the region near the tip is luminous at a quasi-steady corona current. Such a bright spherical region with cylindrical streamers is also clearly visible in Figure 8a.

## 4. Discussion

### Initiation of ball and Cylindrical Streamers

Our study of corona discharges in atmospheric pressure air evidence that (1) both negative and positive coronas develop via the ball streamers near the needle tip at several kilovolts and that (2) positive ball streamers start at

higher voltages and positive cylindrical streamers at lower voltages compared to negative ones.

As already noted, the electric field needed for a negative streamer is two-three times higher than that for a positive one<sup>[27]</sup>. However, in our study, like in others, negative coronas at low voltages were initiated and cylindrical streamers in low electric fields were detected, suggesting two types of corona streamers: ball in high electric fields and cylindrical in more low electric fields. We think that it is the high electric field at needle tips, which provides the initiation of ball streamers.

Figure 11 shows the distribution of electric field strength for needles No. 1a and No. 1b at 2 kV and  $d = 40$  mm.

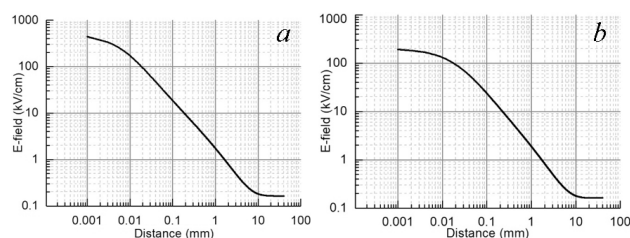


**Figure 11.** Electric field strength versus distance from needles No. 1a (a) and No. 1b (b) at 2 kV,  $d = 40$  mm

From Figure 11 it follows that the electric field strength at the tip of needle No. 1a at 2 kV is higher than 0.4 MV/cm. This value is of the order of the electric field at pointed electrodes in nanosecond pulsed diffuse discharges formed by wide (ball) streamers<sup>[28,31,32]</sup>. Hence, similar mechanisms can be expected for discharges from sharp points at rates of voltage rise of  $<10^6$  V/s and  $>10^{12}$  V/s. The rates  $>10^{12}$  V/s correspond to diffuse discharges involving fast and runaway electrons at negative voltage polarity<sup>[33]</sup> and X rays at positive polarity<sup>[34]</sup>.

Although the electric field for coronas from thin needles is several times lower than the field for nanosecond discharges with pulse amplitudes of tens to hundreds of kilovolts, the time during which their tips is kept at high voltage is much longer. This causes charge accumulation at needle tips, avalanche growth to critical sizes, and ball streamer formation at both voltage polarities.

The emission of electrons from negative tips is more efficient than their emission from positive ones. Besides, nanoparticles<sup>[35]</sup> and dielectric films, including carbon<sup>[36]</sup>, lower the field emission threshold. Therefore, the start voltage of negative coronas is lower.

Under certain conditions, the appearance of primary electrons in length of gaps can be associated with natural background ionizing radiation, which gives  $\sim 10^3$  electron/cm<sup>3</sup> in 1 ns<sup>[27]</sup>, and with dark current, which is recorded at high instrument sensitivity. However, these contributions

are likely important only at positive voltage polarity. With positive needle tips, higher voltages are needed to make the ion concentration sufficient for the start of a positive streamer, suggesting that the generation of primary electrons, in this case, is less efficient. Nevertheless, ball streamers do arise at positive polarity. The motion of ball streamers stops because the electric field decreases rapidly with distance from pointed electrodes and its average value in corona discharges is comparatively small. Under such conditions, the flow of quasi-steady current is provided by charged particle drift in the region of low electric fields and by photoemission via shortwave emission from the plasma that remains as a dense cloud at the tip of a pointed electrode due to its high electric field and ongoing air ionization there. As the voltage of positive polarity at the tip is increased, classical cylindrical streamers start escaping from the plasma cloud, as evidenced by our ICCD imaging. The electric field for the start of cylindrical cathode streamers is much lower and their length is larger than those of negative streamers in corona discharges are.

When cylindrical streamers develop (Figs. 8 and 10), the pulsed current increases greatly (Table 4) due to dynamic displacement current<sup>[28,37]</sup>. As a cylindrical streamer moves from a pointed to a plane electrode kept in a low electric field, capacitive charging occurs between its front and plane electrode. As the voltage is increased, such streamers reach the plane electrode, forming a glow discharge which is further transformed to a spark. Because of the cylindrical streamer formation, the breakdown voltage is lower at positive than at negative voltage polarity.

The current recorded during the formation of ball streamers is also contributed by dynamic displacement current. However, its amplitudes in corona discharges (due to small streamer sizes) are lower than its amplitudes in nanosecond diffuse discharges<sup>[28,37-40]</sup>. Measurement data on electric fields at ionization wave fronts during breakdowns are reported elsewhere<sup>[41-43]</sup>.

## 5. Conclusion

Our research confirms that both negative and positive coronas in atmospheric pressure air develop via ball streamers which appear in the vicinity of electrodes with a small radius of curvature ( $\sim 10$   $\mu$ m). As it follows from calculations, the electric field at the tip of a needle reaches several hundred kilovolts per centimeter at a voltage of a few kilovolts. These conditions approximate those for the generation of fast electrons and X-ray quanta in diffuse discharges<sup>[33]</sup>.

The start voltage of positive streamers, compared to negative ones, is higher due to low initial electron concentrations in air. The lower start voltage of negative stream-



ers is due to more efficient electron emission from metal cathodes. The presence of positive ball streamers suggests that the plasma created at positive needle tips emits short-wave photons, which provide their initiation in a high electric field through air preionization.

At the same voltage, the average current of negative corona with ball streamers are higher and their luminous region is larger than those of positive ones, which can be explained by more efficient electron emission from pointed cathodes and by higher frequencies of Trichel pulses. Their frequency at negative polarity, compared to positive, is more than two orders of magnitude greater.

The average electric field strength for the start of positive cylindrical streamers is two-three times lower than its value for negative ones. When cylindrical streamers start from positive needle tips, the amplitude of current pulses increases greatly, going above their amplitude at negative polarity with the same voltage level. However, in the same conditions, the average current of positive coronas is lower than that of negative ones.

From our study it follows that the ignition of coronas from pointed electrodes of any form and polarity begins with ball streamers due to electric field amplification and that, the initiation of a breakdown at positive polarity is due to cylindrical streamers developing from a plasma cloud near a needle.

Increasing the voltage causes successive discharge transitions from mode to mode. At negative voltage polarity, first comes a dark discharge, and then, a corona with a ball streamer, a corona with steady and pulsed currents, a glow discharge, and a spark. At positive voltage polarity, the sequence of modes includes a dark discharge, a corona with a ball streamer, a quasi-steady corona with rare pulses, a corona with cylindrical streamers, a glow discharge, and a spark. The transition to a glow discharge only little affects the current—voltage characteristic, whereas the transition to a spark involves a steep decrease in the gap voltage and a considerable increase in the amplitude of current pulses.

## Acknowledgments

This work was carried out as part of the project of the Russian Science Foundation no. 18-19-00184.

## References

- [1] L. Léger, E. Moreau, G. G. Touchard. *IEEE T. Ind. Appl.* 2002, 38(6): 1478.
- [2] M. Simek, M. Clupek. *J. Phys. D: Appl. Phys.* 2002, 35(11): 1171.
- [3] Y. S. Akishev, G. I. Aponin, M. E. Grushin, V. B. Karal'nik, M. V. Pan'kin, A. V. Petryakov, N. I. Trushkin. *Plasma Phys. Rep.* 2008, 34(4): 312.
- [4] S. B. Afanas'ev, D. S. Lavrenyuk, I. N. Petrushenko, Y. K. Stishkov. *Tech. Phys.* 2008, 53(7): 848.
- [5] D. Z. Pai, D. A. Lacoste, C. O. Laux, *Jour. Appl. Phys.* 2010, 107(9): 093303.
- [6] M. Sabo, J. Páleník, M. Kučera, H. Han, H. Wang, Y. Chu, Š. Matejčík, *Int. J. Mass Spectrom.* 2010, 293(1-3): 23.
- [7] T. Shao, V. F. Tarasenko, C. Zhang, D. V. Rybka, I. D. Kostyrya, A. V. Kozyrev, P. Yan, V. Y. Kozhevnikov, *New J. Phys.* 2011, 13(11): 113035.
- [8] L. Liu, Z. Zhang, Z. Peng, J. Ouyang, *J. Phys. Conf. Ser.* 2013, 418(1): 012092.
- [9] Y. Zheng, B. Zhang, J. He. *Phys. Plasmas*, 2015, 22(2): 023501.
- [10] X. Li, X. Cui, T. Lu, Y. Liu, D. Zhang, Z. Wang. *IEEE Trans Dielectr Electr Insul.* 2015, 22(2): 1314.
- [11] A. El-Tayeb, A. H. El-Shazly, M. F. Elkady, A. B. Abdel-Rahman. *Plasma Phys. Rep.* 2016, 42(9): 887.
- [12] X. Zhu, L. Zhang, Y. Huang, J. Wang, Z. Liu, K. Yan. *Plasma Sci. Technol.* 2017, 19(7): 075403.
- [13] V. F. Tarasenko, E. K. Baksht, E. A. Sosnin, A. G. Burachenko, V. A. Panarin, V. S. Skakun. *Plasma Phys. Rep.* 2018, 44(5): 520.
- [14] Y. Guan, R. S. Vaddi, A. Aliseda, I. Novosselov. *Phys. Plasmas*, 2018, 25(8): 083507.
- [15] Y. K. Stishkov, A. V. Samusenko, I. A. Ashikhmin. *Phys.-Uspekhi*, 2018, 61(12): 1213.
- [16] R. Bálek and S. Pekárek, *Plasma Sources Sci. T.* 2018, 27(7): 075019.
- [17] Q. Gao, X. Wang, A. Yang, C. Niu, M. Rong, L. Jiao, Q. Ma. *Phys. Plasmas*, 2019, 26(3): 033508.
- [18] B. B. Baldanov, A. P. Semenov, T. V. Ranzhurov, *Bull. Russ. Acad. Sci.: Phys.* 2019, 83(11): 1366.
- [19] Y. Guo, S. Li, Z. Wu, K. Zhu, Y. Han, N. Wang. *Phys. Plasmas*, 2019, 26(7): 073511.
- [20] V. F. Tarasenko, V. S. Kuznetsov, V. A. Panarin, V. S. Skakun, E. A. Sosnin, E. K. Baksht. *JETP Letters*, 2019, 110(1): 85.
- [21] N. G. C. Ferreira, D. F. N. Santos, P. G. C. Almeida, G. V. Naidis, M. S. Benilov, *J. Phys. D: Appl. Phys.* 2019, 52(35): 355206.
- [22] W. Liu, Q. Zheng, M. Hu, L. Zhao, Z. Li. *Plasma Sci. Technol.* 2019, 21(12): 125404.
- [23] Y. Cui, C. Zhuang, R. Zeng, *Appl. Phys. Lett.*, 2019, 115(24): 244101.
- [24] M. Cernak, T. Hoder, Z. Bonaventura. *Plasma Sources Science and Technology.* 2020, 29(1): 013001 .
- [25] L. Li, J. Li, Z. Zhao, C. Li. *Phys. Plasmas*, 2020, 27(2): 023508.
- [26] L. B. Loeb. *Electrical coronas, their basic physical mechanisms*, Univ of California Press, 1965.

- [27] Yu. P. Raizer. Gas Discharge Physics, Berlin: Springer, 1997.
- [28] D. V. Beloplotov, M. I. Lomaev, D. A. Sorokin, V. F. Tarasenko. Phys. Plasmas, 2018, 25(8): 083511.
- [29] G. W. Trichel. Phys. Rev. 1938, 54: 1078.
- [30] V. S. Kuznetsov, V. F. Tarasenko, E. A. Sosnin. Russ. Phys. J. 2019, 62(5): 893.
- [31] G. V. Naidis, V. F. Tarasenko, N. Y. Babaeva, M. I. Lomaev, Plasma Sources Sci. Technol. 2018, 27(1): 013001.
- [32] V. F. Tarasenko, G. V. Naidis, D. V. Beloplotov, I. D. Kostyrya, N. Yu. Babaeva. Plasma Phys. Rep. 2018, 44(8): 746.
- [33] V. F. Tarasenko. Plasma Sources Sci. Technol. 2020, 29(3): 034001.
- [34] C. V. Nguyen, A. P. J. Van Deursen, E. J. M. Van Heesch, G. J. J. Winands, A. J. M. Pemen. J. Phys. D: Appl. Phys. 2009, 43(2): 025202.
- [35] E. Kalered, N. Brenning, I. Pilch, L. Caillault, T. Minéa, L. Ojamäe, Phys. Plasmas, 2017, 24(1): 013702.
- [36] A. Andronov, E. Budylna, P. Shkitun, P. Gabdullin, N. Gnuchev, O. Kvashenkina, A. Arkhipov. Journal of Vacuum Science & Technology B, Nanotechnology and Microelectronics: Materials, Processing, Measurement, and Phenomena, 2018, 36(2): 02C108.
- [37] T. Shao, V. F. Tarasenko, C. Zhang, A. G. Burachenko, D. V. Rybka, I. D. Kostyrya, M. I. Lomaev, E. Kh. Baksht, P. Yan. Rev. Sci. Instrum. 2013, 84(5): 053506.
- [38] S. Chen, L. C. J. Heijmans, R. Zeng, S. Nijdam, U. Ebert. J. Phys. D: Appl. Phys. 2015, 48(17): 175201.
- [39] D. V. Beloplotov, V. F. Tarasenko, D. A. Sorokin, M. I. Lomaev. JETP Lett., 2017, 106(10): 653.
- [40] D. A. Sorokin, V. F. Tarasenko, D. V. Beloplotov, M. I. Lomaev. J. Appl. Phys. 2019, 125(14): 143301.
- [41] J. J. Lowke, F. D'Alessandro. Journal of Physics D: Applied Physics, 2003, 36(21): 2673.
- [42] E. M. Van Veldhuizen, and W. R. Rutgers. J. Phys. D: Appl. Phys. 2003, 36(21): 2692.
- [43] E. Wagenaars, M. D. Bowden, G. M. W. Kroesen. Physical review letters, 2007, 98(7): 075002.